Environmental Science & Technology

pubs.acs.org/est

Open Access

This article is licensed under CC-BY-NC-ND 4.0

Article

Exploring the Androgen Receptor Binding Affinity of Azole Derivatives through Multiscale Computational and Experimental Approaches

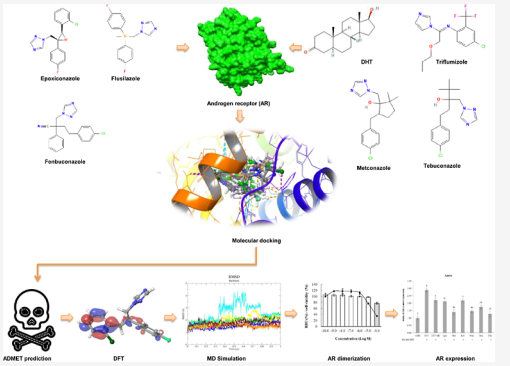
Rajesh Kumar Pathak, Da-Hyun Jeong, Min-Jae Jang, Hee-Seok Lee,* and Jun-Mo Kim*

Cite This: *Environ. Sci. Technol.* 2025, 59, 24323−24334

Read Online

ACCESS | Metrics & More | Article Recommendations | Supporting Information

ABSTRACT: Azoles are widely used in agriculture to combat fungal pathogens and protect crops. However, their increased use in recent years has raised concerns due to their endocrine-disrupting properties and other toxic effects, posing risks to human, animal, and environmental health. This study sought to characterize the interaction between selected azoles and the androgen receptor (AR) and to assess their impact on the receptor's normal activity. Molecular docking was performed with azoles and dihydrotestosterone (DHT) as reference ligand, followed by molecular mechanics/generalized born surface area (MM/GBSA) analysis of the docked complexes to evaluate their binding affinity with AR. ADMET analysis was conducted for all compounds along with density functional theory calculations, molecular dynamics simulations (MDS), and post-MDS MM/GBSA binding energy calculations for the top six azoles, including DHT, to assess their toxicity, chemical reactivity, structural and conformational stability, mobility, interaction patterns, and binding affinity. Additionally, experimental studies of the top six azoles, based on their affinity for AR, revealed that they inhibited the dimerization of DHT-bound ARs in the cytoplasm and suppressed DHT-induced AR expression. These findings underscore the importance of developing targeted strategies to mitigate the reproductive toxicity of azoles and promote environmental health.



KEYWORDS: *azoles, androgen receptor, environmental health, molecular docking, molecular dynamics simulations, BRET*

Downloaded via CHUNG-ANG UNIV on December 15, 2025 at 04:18:39 (UTC).
See https://pubs.acs.org/sharingguidelines for options on how to legitimately share published articles.

1. INTRODUCTION

Plant breeding methods and biotechnology are advancing the development of disease-resistant and high-yield crop varieties. However, the use of pesticides is still necessary to protect crops from various diseases, including those caused by emerging pathogens and the impacts of climate change.[1] The continued reliance on pesticides has raised concerns about their effects on human, animal, and environmental health.[2−5] Azole pesticides, in particular, have been extensively used to protect crops from fungal infections since the 1970s. Currently, approximately 25 different azole compounds are used as fungicides for crop protection, holding a significant market share of 20% to 25% in the global fungicide market.[5−7] Additionally, azoles are widely used in human medicine as antifungal agents. However, their frequent use in both agriculture and medicine has contributed to the growing problem of azole fungicide resistance.[8]

Like many other chemicals, azoles can inadvertently impact human, animal, and environmental health, with growing concerns over their toxicity and endocrine-disrupting effects.[6] Their primary antifungal mechanism involves inhibiting the 14α-demethylase enzyme (CYP51) in the fungal cell membrane.[5,9] However, this disruption can also lead to undesirable effects on the human endocrine system by interfering with the CYP19 enzyme (aromatase), which converts androgens into estrogens during steroidogenesis.[10] Moreover, numerous studies have shown that azole antifungals, particularly those containing imidazoles and conazoles, have endocrine-disrupting effects mediated by hormone receptors. As a result, azole fungicides may negatively affect mammalian reproductive and developmental systems, which depend on the steroid hormone pathway.[5,11] It also raises concerns about fetal exposure during pregnancy, potentially leading to long-term reproductive issues in offspring.[12] Additionally, pan-azole-resistant *Aspergillus fumigatus* strains from tulip cultivation sites have been found to spread through clonal expansion and have also developed resistance to multiple fungicides, including azoles. This gives them a survival edge in fungicide-rich environments and raises concerns about their potential impact on human health.[13,14]

Received: August 5, 2025
Revised: October 14, 2025
Accepted: October 15, 2025
Published: November 6, 2025



© 2025 The Authors. Published by American Chemical Society

Given the documented toxicity and widespread use of azoles, it is crucial to understand how they interact with human proteins.[9,15] Considering their endocrine-disrupting behavior, it is equally important to investigate how they interact with critical receptors such as androgen and estrogen receptors.[4,5] This knowledge can raise awareness and promote the search for alternative solutions to protect environmental health in the future. Conventional methods for studying the interactions between toxic chemicals and human molecular targets primarily involve experimental techniques, including in vitro binding assays, cell culture studies, and animal model experiments.[4,16] These methods allow for direct observation of how toxic chemicals bind to specific receptors or proteins and assess their subsequent effects on cellular functions and overall health. However, traditional methods are often time-consuming, costly, and resource-intensive[17,18] and may not fully capture the complexity of these interactions.[4,18] To address these limitations, computational toxicology approaches have emerged as valuable tools for decoding these interactions.[19,20] With advances in software and algorithms, understanding the behavior and interaction of toxic chemicals has become easier, reducing the need for in vitro experiments, saving time and costs, and ultimately contributing to the development of policies aimed at protecting environmental health.[18,19,21]

Considering the endocrine-disrupting behavior of azoles through their interaction with the androgen receptor (AR), it is crucial to decode and visualize these interactions as this remains a significant area of scientific research. This is particularly important given the growing recognition of azoles' potential impacts on both environmental and human health.[6,12] Previous research has established the widespread presence of azoles in the environment with resistant *A. fumigatus* strains detected in environmental samples worldwide,[22] along with their strong endocrine-disrupting effects particularly antiandrogenic activity mainly characterized through reporter gene assays and binding affinity measurements.[12] However, several critical gaps remain. The contributions of specific amino acid residues to azole derivatives with AR binding have not yet been determined. Density function theory (DFT)-based reactivity profiling, including analysis of electronic parameters such as frontier molecular orbitals, has not been explored, even though it could help uncover quantum chemical drivers of azoles−AR antagonism. The dynamic stability of AR−azole complexes has also not been examined through molecular dynamics simulations (MDS). Moreover, a systematic comparative analysis of binding free energies (ΔG) across different azole chemotypes is lacking. Experimental validation of the computational findings has likewise not been systematically applied to azole compounds. This study addresses these gaps through an integrated computational and experimental approach. Investigating these aspects is vital for raising public health awareness as it will help minimize potential adverse effects and better inform safety guidelines for these compounds.

Beyond their prominent share among fungicides, azoles should be considered within the broader pesticide landscape. Global use data indicate that fungicides and bactericides constitute a substantial portion of the total pesticide inputs in many agricultural regions. For example, the worldwide agricultural use of fungicides and bactericides is predicted to increase from approximately 1.01 million metric tons in 2023 to nearly 1.05 million metric tons by 2027 (https://www.statista.com/statistics/1403201/global-agricultural-use-of-fungicides-and-bactericides-forecast/accessed on 07/09/2025). In contrast, insecticides, which target arthropod pests, represent a significant portion of pesticide use, with neonicotinoids and organophosphates frequently detected in environmental and human exposure studies.[23] For example, herbicides dominate drinking water contamination, contributing 55% to total pesticide concentrations, while insecticides are the most abundant group in indoor dust and urine samples.[23] Framing azole exposure relative to insecticide usage clarifies the ecological scope of endocrine-active chemical mixtures encountered in agroecosystems and human exposure pathways such as diet and dust.[23,24] Accordingly, comparing azole usage with insecticide application volumes helps contextualize the potential footprint of AR active azoles, particularly given their persistence in aquatic systems and synergistic effects with other pesticides.[23,24]

Given the reported hazardous and endocrine-disrupting nature of azoles, 19 specific compounds were selected for this study.[6,9,15] Our primary objective is to elucidate their molecular interactions with the AR using an integrated computational and experimental approach. Computationally, we employ molecular docking, MM/GBSA binding free-energy calculations, DFT analysis, and MD simulations to predict binding modes, affinities, key residues, electronic properties, and complex stability. The top-ranking compounds identified computationally are then subjected to experimental validation using BRET assays, quantitative RT-PCR, and protein expression analysis. This combined strategy allows us to characterize the binding mechanisms of these azoles with AR and assess their functional consequences.

2. MATERIALS AND METHODS

2.1. Azole Structure Retrieval and Preparation. The structures of azoles were obtained from the PubChem database (https://pubchem.ncbi.nlm.nih.gov/) and processed using the LigPrep module of Schrödinger Maestro.[25] Energy minimization was carried out using the OPLS4 force field.[26] LigPrep converts 2D structures into 3D structures by adding hydrogens, adjusting bond lengths and angles, and selecting the lowest-energy conformer, taking into account the correct chiralities, tautomers, stereochemistries, and ring conformations. All possible protonation states, ionization states, tautomers, stereochemistries, and ring conformations were generated by using the default ionization state parameter in Epik. Stereoisomers were generated using default parameters with a maximum of 32 stereoisomers per ligand. For each ligand, only the lowest-energy conformation was selected.

2.2. Protein Preparation and Receptor Grid Generation for AR. The three-dimensional structure of the AR in its agonist conformation, complexed with DHT was obtained from the Protein Data Bank (PDB ID: 1T63) (https://www.rcsb.org).[27] The AR PDB file was processed using the Protein Preparation Wizard in Schrödinger Maestro, which removed water molecules, added hydrogen atoms, completed missing loops, capped termini, adjusted charge states, and corrected hydrogen bond assignments. The protein was then minimized using the OPLS4 force field.[26] Receptor grid generation was carried out with default parameters using the Glide-receptor grid generation module, employing a van der Waals radius scaling factor of 1.0 and a partial charge cutoff of 0.25. The receptor grid was generated based on the cocrystallized ligand

https://doi.org/10.1021/acs.est.5c10722
Environ. Sci. Technol. 2025, 59, 24323−24334

DHT in the AR binding site, with the grid centered on the ligand for molecular docking.

2.3. Molecular Docking and Pre-MDS MM/GBSA Binding Energy Calculations. Molecular docking of azoles and the cocrystallized ligand DHT with AR was performed using the Glide module in Schrödinger, following the standard precision (SP) protocol with default settings.[28] For precise binding energy calculations, molecular mechanics/generalized born surface area (MM/GBSA) analyses were conducted on the docked complexes generated by Glide. The binding energy (ΔG bind) was calculated using the Prime-MM/GBSA module in Schrödinger, applying the volume surface generalized born solvation model and OPLS4 force field.[26]

2.4. Pharmacokinetics Analysis and Toxicity Risk Prediction. To enable a comprehensive risk assessment alongside binding affinity data, the ADMET properties of the azoles and DHT were evaluated. ADME predictions were performed using the QikProp module in Schrödinger Maestro.[25] Toxicity profiles were predicted using the pkCSM tool.[29] These analyses assessed potential off-target effects and bioavailability, which influence the potential of the compounds to reach their molecular targets.

2.5. DFT Analysis. DFT calculations were conducted to assess the chemical reactivity of the top-screened azoles compared to DHT. These calculations focused on identifying the frontier molecular orbitals, specifically the highest occupied molecular orbital (HOMO) and the lowest unoccupied molecular orbital (LUMO), to gain insights into how azoles interact with the AR. DFT calculations employed the B3LYP-D3 functional and the 6-31G** basis set using the Jaguar module in Schrödinger Maestro.[25,30]

2.6. MDS Analysis. To evaluate the dynamic behavior of AR before and after ligand binding, MDS were conducted on AR and the top-screened AR-azole complexes, including flusilazole, epoxiconazole, fenbuconazole, triflumizole, and metconazole, alongside the AR-DHT complex. The simulations were carried out using the Desmond MD engine in Schrödinger. The system was solvated using a TIP3P water model within an orthorhombic periodic boundary box, with dimensions uniformly set to 10 Å along each axis and fixed angles at 90°.[31,32] Chloride ions (Cl^-) were added to neutralize the charge. All other parameters, such as bond lengths and angles, were set to their default values. The system, including AR and its docked complexes, was simulated using the OPLS4 force field.[26] The minimized model underwent MDS for 1 μs within the *NPT* ensemble at a constant temperature of 300 K and a pressure of 1.01325 bar. Trajectories generated from the simulations were analyzed using the simulation interaction diagram module in Desmond to investigate the behavior and interactions of the selected compounds with the AR.

2.7. Post-MDS MM/GBSA Binding Energy Calculations. Post-MDS binding energy calculations were performed by using the MM/GBSA method. The ΔG_{bind} for the top-screened AR-azole complexes (AR-flusilazole, AR-epoxiconazole, AR-fenbuconazole, AR-triflumizole, AR-metconazole, and AR-tebuconazole) and the reference AR-DHT complex was calculated using the Schrödinger Python script thermal_mmgbsa.py. This script processed the MD trajectory from Desmond, analyzing 1000 snapshots from a 1 μs simulation through MM/GBSA analysis. The analysis focused on van der Waals interactions, Coulombic energy, hydrogen bonding contributions, lipophilic energy, $\pi-\pi$ stacking energy, Generalized Born electrostatic solvation energy, and total binding free energy (ΔG_{bind}).[25,32]

2.8. BRET Assay for AR Dimerization. The inhibition of azole-induced dimerization of ligand-bound ARs in the cytoplasm was confirmed using a BRET-based in vitro assay, which was validated in our previous study.[33] Briefly, BRET signals from the dimerization of cytosolic DHT-bound ARs were measured in the presence and absence of azoles. The detailed protocol for the assay is provided in Supporting Information SI 1.

2.9. Quantitative RT-PCR for AR mRNA Expression. The quantity of total RNA was determined through the utilization of a quantitative real-time polymerase chain reaction system incorporating TaqMan primers (Applied Biosystems, USA). This was conducted after the synthesis of RNA into cDNA using GRKO cell lines. 22Rv1/MMTV-GRKO cells were used as a model for human nuclear receptor signaling.[34] These cells are deficient in endogenous glucocorticoid receptor (GR) signaling and exhibit low background expression of other steroid receptors, minimizing GR-mediated cross-talk and nonspecific steroid receptor activity. Consequently, they provide a sensitive and specific system for analysis of transfected human AR activity by qPCR and Western blot.[35,36] The protocol for this procedure is described in Supporting Information SI 2.

2.10. Western Blot Analysis for AR Protein Expression. DHT-induced AR protein expression was assessed in the presence and absence of azoles via Western blot analysis. The protocol for this procedure is described in Supporting Information SI 3.

3. RESULTS

3.1. Molecular Docking and Binding Energy Calculations of Azoles with AR. This study highlights the interactions of selected azoles with the AR through molecular docking and binding energy calculations. To assess the strength of these interactions, we first calculated the binding free energy of the cocrystallized ligand DHT with AR. The docking score of DHT was determined to be −12.590 kcal/mol, indicating strong binding affinity, as lower binding energies generally suggest stronger interactions between a ligand and its target. The docking scores of the selected azole compounds were as follows: flusilazole, −9.416 kcal/mol; epoxiconazole, −9.064 kcal/mol; fenbuconazole, −8.891 kcal/mol; triflumizole, −8.734 kcal/mol; metconazole, −7.969 kcal/mol; tebuconazole, −7.798 kcal/mol; paclobutrazol, −7.794 kcal/mol; hexaconazole, −7.605 kcal/mol; triadimefon, −7.519 kcal/mol; tricyclazole, −7.366 kcal/mol; myclobutanil, −7.315 kcal/mol; triadimenol, −7.301 kcal/mol; thiabendazole, −7.014 kcal/mol; tebufenpyrad, −6.864 kcal/mol; cyproconazole, −6.702 kcal/mol; carbendazim, −6.371 kcal/mol; cafenstrole, −6.211 kcal/mol; benomyl, −5.933 kcal/mol; and thiophanate-methyl, −5.074 kcal/mol. To further validate these docking results, MM/GBSA binding free energy calculations were performed for all docked complexes. The predicted binding free energies were as follows: DHT (−85.29 kcal/mol), flusilazole (−44.25 kcal/mol), epoxiconazole (−52.94 kcal/mol), fenbuconazole (−61.65 kcal/mol), triflumizole (−50.08 kcal/mol), metconazole (−48.65 kcal/mol), tebuconazole (−40.67 kcal/mol), paclobutrazol (−43.88 kcal/mol), hexaconazole (−41.08 kcal/mol), triadimefon (−47.26 kcal/mol), tricyclazole (−34.57 kcal/mol), myclobutanil (−42.00 kcal/mol), triadimenol (−41.34 kcal/mol), thiaben-

https://doi.org/10.1021/acs.est.5c10722
Environ. Sci. Technol. 2025, 59, 24323−24334

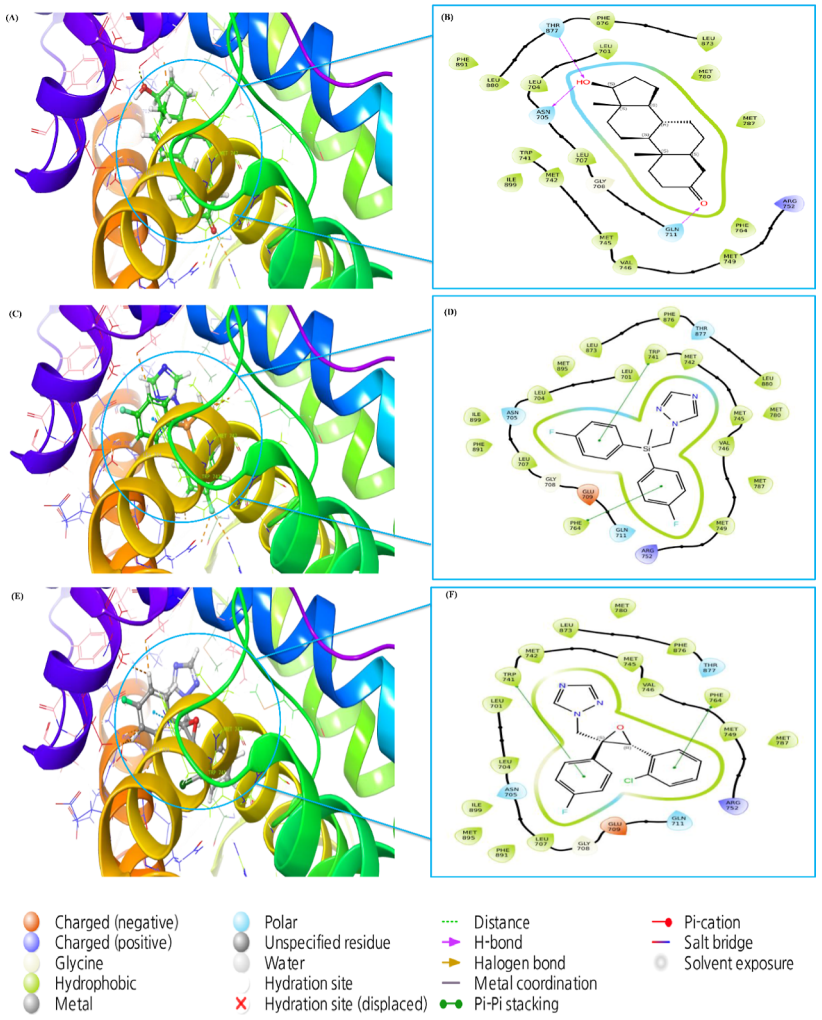


Figure 1. Interactions of DHT (A,B) and azoles (C,D) flusilazole and (E,F) epoxiconazole with the AR. Key amino acid residues involved in protein−ligand interactions are depicted as predicted by molecular docking. Both 2D and 3D representations are presented, with the legend for the 2D images included within the figure.

dazole (−33.34 kcal/mol), tebufenpyrad (0.89 kcal/mol), cyproconazole (−41.80 kcal/mol), carbendazim (−32.64 kcal/mol), cafenstrole (−3.74 kcal/mol), benomyl (−36.87 kcal/mol), and thiophanate-methyl (−36.50 kcal/mol). Our findings revealed that DHT has the highest binding affinity with AR, consistent with its role as a natural ligand. However, flusilazole displayed the strongest binding affinity among the tested azoles. The detailed binding energies and interacting amino acid residues for AR are summarized in Table S1 (see Table S1, Supporting Information). Additionally, the protein−ligand interaction diagrams are shown in Figures 1 and S1 (see Figure S1, Supporting Information).

3.2. Analysis and Prediction of Physicochemical Properties and Toxicity. The pharmacokinetic and toxicity performance parameters of the selected azole compounds were evaluated using the QikProp module within Schrödinger. The predicted molecular weights ranged from 189.234 to 350.435 Da. The following physicochemical parameters were also assessed: hydrogen bond donors varied from 0 to 2, hydrogen bond acceptors varied from 2 to 8.5, QPlogPo/w from 1.038 to 4.881, QPlogS from −5.982 to −1.358, QPPCaco from 472.643 to 4236.086, QPPMDCK from 332.297 to 10,000, and QPlogBB from −0.865 to 0.258. All compounds complied with Lipinski's Rule of Five and the Rule of Three, with only tebufenpyrad and thiophanate-methyl violating the Rule of Three. The predicted percentage of human oral absorption for DHT and most azoles was 100%, except for carbendazim, cafenstrole, benomyl, and thiophanate-methyl. Detailed values for each compound are presented in Supporting Information Table S2.

Toxicity predictions were conducted by using the pkCSM tool. AMES toxicity was identified for epoxiconazole, triflumizole, myclobutanil, thiabendazole, tebufenpyrad, cyproconazole, carbendazim, benomyl, and thiophanate-methyl. The predicted values for oral rat acute toxicity ranged from 1.783 to 2.901 mol/kg, while oral rat chronic toxicity values ranged from 0.614 to 1.872 log mg/kg_bw/day. Hepatotoxicity was predicted for tebuconazole, triadimefon, tricyclazole, tebufenpyrad, carbendazim, cafenstrole, and benomyl. Detailed information on these predictions is provided in Supporting Information Table S3.

3.3. DFT Calculations. The frontier molecular orbitals, specifically the HOMO and LUMO, of the top six azoles based on their binding free energy with the AR were analyzed using DFT, with DHT serving as a reference. This analysis was conducted utilizing the Jaguar module in Schrödinger to estimate orbital energies and evaluate the chemical reactivity potential of each ligand. Figure S2 illustrates the orbital

https://doi.org/10.1021/acs.est.5c10722
Environ. Sci. Technol. 2025, 59, 24323−24334

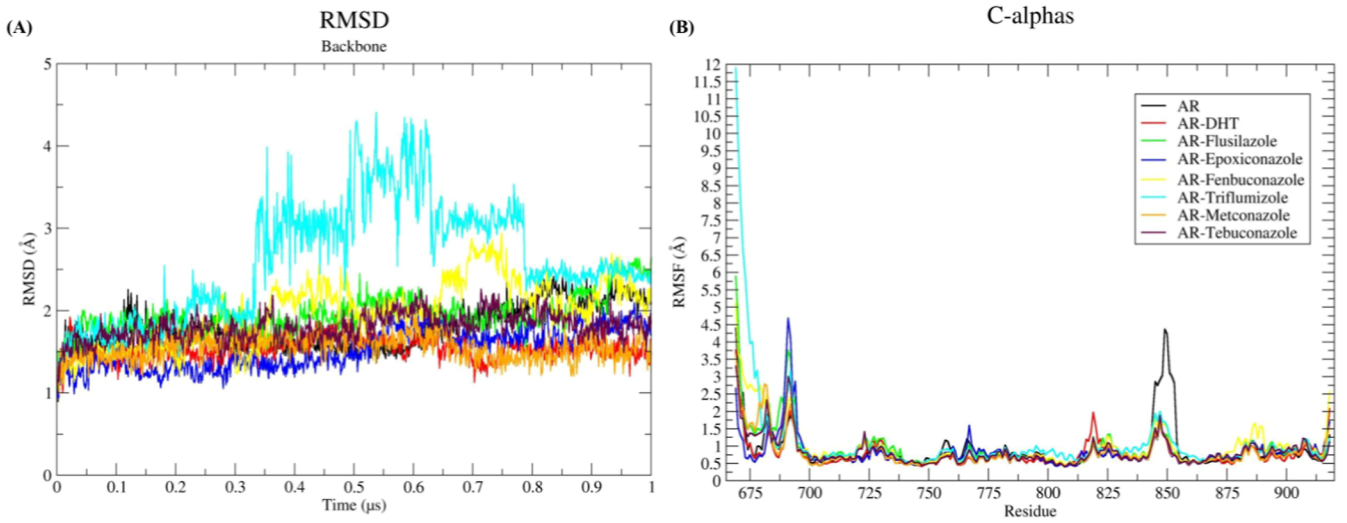


Figure 2. Structural stability and flexibility of the AR before and after ligand binding, as assessed through 1 μs of MDS. (A) The rmsd of the AR backbone shows an initial increase, indicating equilibration of the AR structure, followed by a stable phase, which suggests overall structural stability. (B) RMSF of each residue in the AR ligand-binding domain. The RMSF values reflect the flexibility of individual residues, with higher values indicating greater atomic fluctuations.

distributions, and Table S4 presents calculated HOMO−LUMO energy gaps. A broader energy gap within a molecule generally indicates greater chemical stability and lower reactivity, while a narrower energy gap is associated with decreased stability and increased reactivity as electron transitions occur more readily. Among the compounds studied, tebuconazole and metconazole exhibited the largest energy gaps (6.15 and 6.10 eV, respectively), suggesting higher chemical stability. In contrast, triflumizole displayed the narrowest gap (4.92 eV), indicating comparatively higher reactivity. Interestingly, triflumizole also demonstrated prominent fluctuations in MD simulations and altered AR geometry, suggesting that its higher reactivity may influence receptor dynamics. Although the differences in energy gaps are moderate, they may contribute to differences in binding kinetics or conformational impact upon receptor engagement. The relatively lower HOMO−LUMO gaps in some azoles compared to DHT (6.04 eV) could reflect their potential to participate in charge transfer or electron-donating/accepting interactions, which may partially explain their antagonistic effects on AR. Thus, DFT-based reactivity descriptors support and complement the docking and simulation findings by offering a quantum chemical perspective on ligand behavior. Detailed results are provided in Supporting Information, Table S4.

3.4. MD Simulation for Exploring Structural Stability, Flexibility, and Binding Interaction. MD simulations were performed to investigate the dynamic characteristics of the AR both in its unbound state and when bound to various azoles, using DHT as a reference. Key parameters were analyzed to understand the nature and dynamic behavior of the AR. The stability of AR was assessed through root-mean-square deviation (rmsd) analysis of the MD simulation trajectories, where lower rmsd values indicate a more stable complex. rmsd was measured over 1 μs to evaluate structural deviations over time. Both AR and all selected docked complexes exhibited low rmsd values, indicating stable interactions. Additionally, the AR−triflumizole complex showed more fluctuations compared to those of the other complexes; however, it stabilized after 800 ns. The average rmsd for AR was calculated to be 1.79 Å, while the rmsd values for the complexes AR-DHT, AR-flusilazole, AR-epoxiconazole, AR-fenbuconazole, AR-triflumizole, AR-metconazole, and AR-tebuconazole were 1.53, 1.95, 1.52, 1.97, 2.59, 1.55, and 1.79 Å, respectively. These data suggest that all selected complexes were well-equilibrated throughout the simulation. However, the AR-triflumizole complex exhibited an rmsd greater than 4 Å between 350 and 600 ns, which decreased after 600 ns and stabilized after 800 ns. Overall, the analysis indicates that all systems appeared to be well-equilibrated and formed stable complexes (Figure 2A).

Root-mean-square fluctuation (RMSF) analyses provided insights into the flexibility and mobility of amino acid residues within AR and its complexes with different azoles and DHT over a 1 μs duration. The average RMSF of the AR was found to be 0.87 Å. The calculated RMSF values for AR bound with DHT, flusilazole, epoxiconazole, fenbuconazole, triflumizole, metconazole, and tebuconazole were 0.76, 0.94, 0.83, 0.97, 1.10, 0.80, and 0.83 Å, respectively. Higher RMSF values were observed in the AR−triflumizole complex, suggesting ligand-induced changes in the receptor geometry. A detailed residue-wise RMSF analysis revealed notable fluctuations in the region spanning Cys669 to Val684. This segment, located near the entrance of the ligand-binding domain, exhibits increased flexibility that may contribute to conformational changes affecting the AR function. Additionally, moderate fluctuations were observed around residues 690−695, which may reflect localized structural perturbations induced by triflumizole binding (Figure 2B).

AR interactions with ligands were monitored throughout the simulation and categorized into hydrogen bonds, hydrophobic interactions, ionic interactions, and water bridges. Our analysis indicated that DHT forms more hydrogen bonds with AR compared to the azoles. Specifically, DHT maintained a hydrogen bond with AR Asn705 throughout the simulation. Additionally, hydrogen bonds with Thr877, Gln711, and Arg752 were sustained for over 90%, 10%, and 5% of the simulation time, respectively. DHT also established hydrophobic, ionic, and water bridge interactions (Figures S3A and S4A, Supporting Information). During the MD simulation,

https://doi.org/10.1021/acs.est.5c10722
Environ. Sci. Technol. 2025, 59, 24323−24334

Table 1. Predicted Binding Free Energies (kcal/mol) Obtained via Post-MDS MM/GBSA Calculations for DHT and Azole Compounds[a]

compound name	DHT	flusilazole	epoxiconazole	fenbuconazole	triflumizole	metconazole	tebuconazole
ΔG_{vdw}	−48.16	−46.03	−48.76	−52.49	−51.65	−51.46	−51.03
ΔG_{coul}	−20.53	−5.21	−5.74	−7.39	−5.64	−16.89	−11.83
ΔG_{Hbond}	−0.66	−0.07	−0.17	−0.10	−0.01	−0.00	−0.00
ΔG_{Lipo}	−27.38	−22.84	−29.80	−28.06	−21.13	−29.81	−27.42
ΔG_{Pack}	0	−1.56	−2.02	−1.95	−0.97	−1.54	−1.96
ΔG_{SolGB}	20.68	17.78	17.71	20.77	15.40	25.54	22.73
ΔG_{bind}	−75.03	−56.70	−67.60	−67.76	−62.38	−73.40	−67.91

[a] ΔG_{vdw}: contribution of van der Waals interaction energy to binding free energy; ΔG_{coul}: contribution of Coulombic energy to binding free energy; ΔG_{Hbond}: contribution of hydrogen bonding to binding free energy; ΔG_{Lipo}: contribution of lipophilic energy to binding free energy; ΔG_{Pack}: contribution of $\pi-\pi$ packing energy to binding free energy; ΔG_{SolGB}: contribution of generalized Born electrostatic solvation energy to binding free energy. ΔG_{bind}: total binding free energy.

flusilazole, epoxiconazole, fenbuconazole, triflumizole, metconazole, and tebuconazole exhibited a higher propensity for hydrophobic interactions than DHT. Flusilazole interacted with Gln783 through hydrogen bonding, maintaining this interaction for over 10% of the simulation time, while other residues interacted for 0 to 70% of the simulation time (Figure S3B). Epoxiconazole was shown to interact with Ser778 and Gln783 via hydrogen bonds for over 20% and approximately 5% of the simulation time, respectively, with other residues maintaining interactions for 0 to 50% of the simulation time (Figure S3C). Fenbuconazole maintained hydrogen bond interactions with Gln711 and Arg752 for around 2% and 4% of the simulation time, respectively, while other residues exhibited hydrophobic and water bridge interactions for 0 to over 60% of the simulation time (Figure S3D). Triflumizole maintained a hydrogen bond with Asn705 for about 1% of the simulation time, while other residues maintained hydrophobic and water bridge interactions for 0 to 70% of the simulation time (Figure S4B). Metconazole sustained a hydrogen bond interaction with Thr877 for over 70% of the simulation time, while other residues exhibited hydrophobic interactions for 0 to over 70% of the simulation time (Figure S4C). Tebuconazole maintained a hydrogen bond interaction with Asn705 for more than 70% of the simulation time, along with a shorter interaction with Thr877. Other residues maintained interactions through hydrophobic and water bridge interactions for 0 to 60% of the simulation time. Notably, most interacting residues were found to be common among the ligands, which may influence the natural interactions between DHT and AR (Figure S4D).

3.5. Post-MDS MM/GBSA Binding Energy Calculations of Azoles with AR Using MD Simulation Trajectories. To strengthen the findings from the MD simulations, we computed the binding free energy (ΔG_{bind}) across the entire MD trajectory for all complexes generated over 1 μs of simulation time. This comprehensive analysis provides a detailed assessment of the binding affinity. Using post-MD MM/GBSA calculations, we derived the ΔG_{bind} values, as detailed in Table 1. The predicted average binding energy of DHT with AR was found to be the lowest at −75.03 kcal/mol, compared to the azoles, as DHT is the natural ligand of AR. The binding energies for the azoles were as follows: flusilazole (−56.70 kcal/mol), epoxiconazole (67.60 kcal/mol), fenbuconazole (67.76 kcal/mol), triflumizole (62.38 kcal/mol), metconazole (73.40 kcal/mol), and tebuconazole (−67.91 kcal/mol). Among these, metconazole exhibits the highest affinity for AR, as predicted by the post-MD MM/GBSA calculations. Additionally, other relevant energies were calculated and are provided in Table 1. Based on the post-MD MM/GBSA binding free energies (ΔG_{bind}), the binding affinity of the studied compounds for AR can be ranked as follows: DHT > metconazole > tebuconazole ≈ fenbuconazole > epoxiconazole > triflumizole > flusilazole. Overall, these computational predictions indicate that azoles maintain interactions with AR that may affect its normal functions.

3.6. Inhibiting DHT-Induced Dimerization of Cytosolic ARs by Azoles. To evaluate the impact of azoles on androgen-induced dimerization of cytosolic ARs, we measured the BRET signals induced by DHT in the presence of six azoles: flusilazole, epoxiconazole, fenbuconazole, triflumizole, metconazole, and tebuconazole, along with the AR antagonist flutamide. Initially, a range-finding test was conducted on a logarithmic scale to confirm the intrinsic toxicity of the azoles and their potential to inhibit DHT-induced dimerization. Subsequently, a comprehensive test was performed in a 1:1 ratio to investigate the suppressive effects of the six azoles on DHT-induced dimerization of cytosolic ARs. The results indicated that all six azoles inhibited DHT-induced dimerization at noncytotoxic concentrations (Table S5 and Figure 3). The AR antagonist bicalutamide also demonstrated an inhibitory effect on DHT-induced dimerization, with IC_{30} and IC_{50} values of 5.62×10^{-7} and 2.76×10^{-6} M, respectively (Figure 3A).

3.7. Expression of AR mRNAs by Azoles. The effects of six azoles on DHT-induced AR mRNA were evaluated, showing that all six azoles significantly reduced AR mRNA levels. As shown in Figure 4, the reduction in AR mRNA levels for each azole compared to the DHT-only treatment group was as follows: epoxiconazole (59.0%), fenbuconazole (45.0%), flusilazole (60.4%), metconazole (27.8%), tebuconazole (37.5%), and triflumizole (26.5%). The inhibitory effects of epoxiconazole and flusilazole were not significantly different from the positive control group treated with bicalutamide (62.5%). Specifically, metconazole and triflumizole demonstrated inhibition levels similar to those of the vehicle control group.

3.8. Suppression of DHT-Induced AR Protein Expression by Azoles. The effects of azoles on DHT-induced AR protein expression were assessed, revealing that all six azoles significantly suppressed AR expression (Figure 5). As shown in Figure 5 (B), the suppression levels for each azole were as follows: flusilazole (26.7%), epoxiconazole (51.3%), fenbuconazole (24.6%), triflumizole (49.6%), metconazole (39.7%), and tebuconazole (55.9%), all compared with the DHT-only treatment group. Notably, the inhibition levels of

https://doi.org/10.1021/acs.est.5c10722
Environ. Sci. Technol. 2025, 59, 24323−24334

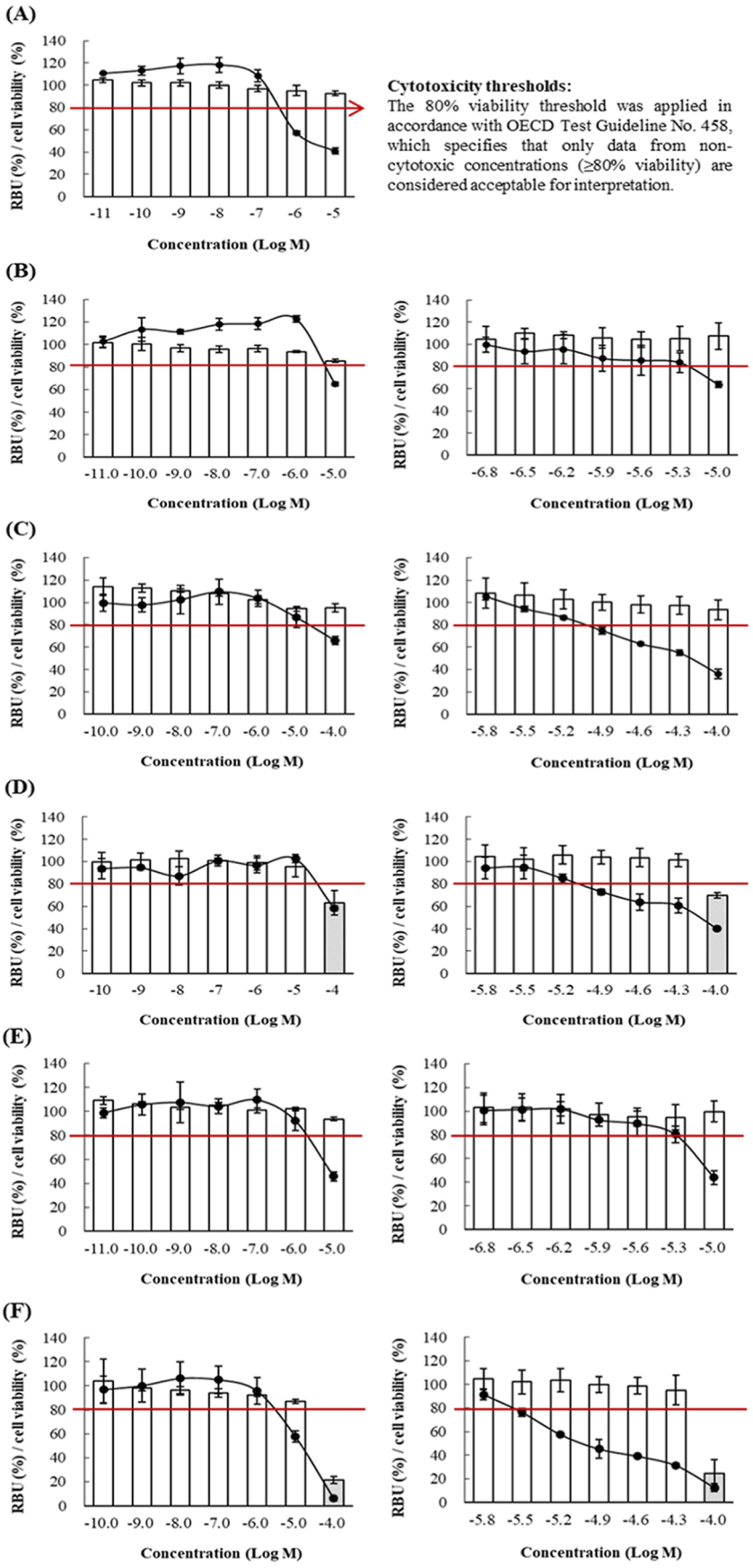


Figure 3. continued

https://doi.org/10.1021/acs.est.5c10722
Environ. Sci. Technol. 2025, 59, 24323−24334

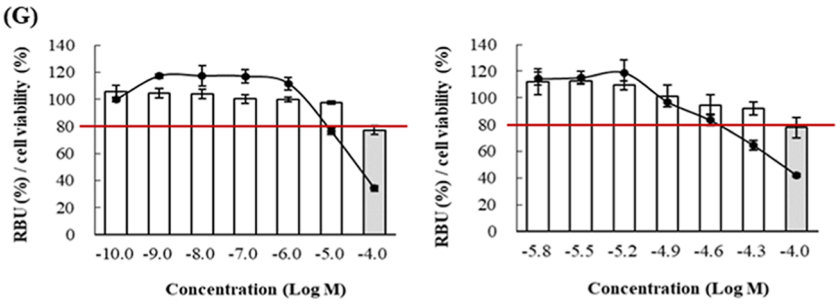


Figure 3. Concentration response curves induced by the positive control (bicalutamide, A) and azoles: flusilazole (B), epoxiconazole (C), fenbuconazole (D), triflumizole (E), metconazole (F), and tebuconazole (G) in the presence of 800 pM DHT. BRET signals are expressed as a percentage of the signal response to 800 pM DHT (±standard deviation). Gray areas indicate cell viability below 80.0%.

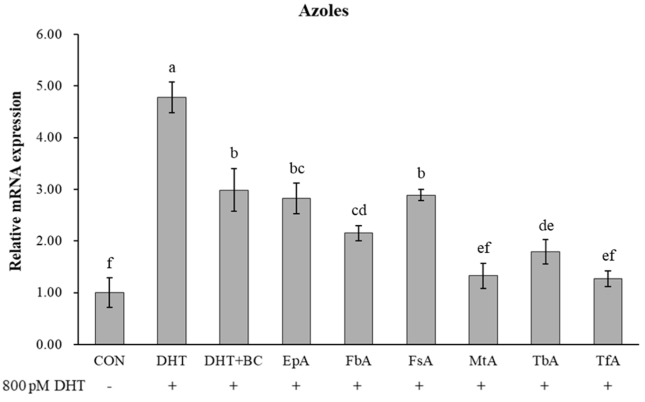


Figure 4. Expression of total AR mRNA treated with DHT in the presence of six azole compounds. Values are expressed as the mean ± standard deviation (SD) (n = 3). BC: bicalutamide, EpA: epoxiconazole, FbA: fenbuconazole, FsA: flusilazole, MtA: metconazole, TbA: tebuconazole, TfA: triflumizole. Statistical analysis was performed using one-way ANOVA followed by Tukey's post hoc test at a 95% confidence level. Groups sharing at least one letter (a−f) are not significantly different, whereas groups with no shared letters differ significantly ($p < 0.05$). All statistical analyses were conducted using GraphPad Prism (version 8.0).

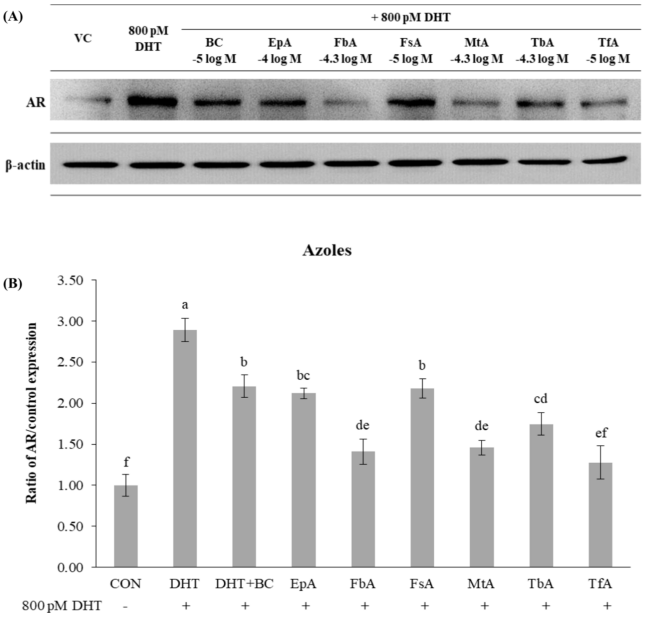


Figure 5. Expression of whole AR proteins treated with DHT in the presence of six azole compounds. Band intensities were quantified from the Western blot shown in (A) and normalized to the vehicle control group (B). Values are expressed as the mean ± standard deviation (SD) (n = 3). BC: bicalutamide, EpA: epoxiconazole, FbA: fenbuconazole, FsA: flusilazole, MtA: metconazole, TbA: tebuconazole, and TfA: triflumizole. Statistical analysis was performed using one-way ANOVA followed by Tukey's post hoc test at a 95% confidence level. Groups sharing at least one letter (a−f) are not significantly different, whereas groups with no shared letters differ significantly ($p < 0.05$). All statistical analyses were conducted using GraphPad Prism (version 8.0).

fenbuconazole, metconazole, tebuconazole, and triflumizole were significantly greater than those of the positive control group treated with bicalutamide. Triflumizole, in particular, demonstrated a suppression level comparable to that of the vehicle control group.

4. DISCUSSION

Despite their effectiveness, the widespread use of azoles raises concerns about their impact on human, animal, and environmental health.[37] Numerous studies involving rats and mice have explored the endocrine-disrupting effects of azole fungicides, revealing a range of adverse reproductive outcomes. Notably, several azoles have been shown to exhibit antiandrogenic effects, such as a shortened anogenital distance (AGD) in male offspring following developmental exposure.[12,38] Interestingly, some azole fungicides can even lead to longer AGDs in both male and female offspring.[12,39] Developmental exposure to azoles has also been linked to nipple retention in male rat offspring, a biomarker for impaired androgen action.[12,40] Additionally, these compounds have been associated with an increased occurrence of malformed external genitalia, delayed onset of puberty, and reduced sperm motility.[12,38]

Given their harmful effects, exploring how azoles interact with human targets is crucial to visualize and understand these interactions.[41,42] Approaches based on computational toxicology, combined with experimental studies such as BRET-based assays, hold significant promise for elucidating molecular interactions.[20,43] Considering the endocrine-disrupting properties of azoles, we conducted molecular docking studies to investigate their interactions with the AR, identifying the specific amino acid residues involved and comparing the binding energies of azole compounds to those of the natural ligand, DHT. Well-characterized AR antagonists such as flutamide were not included as controls in the current docking and simulation analyses as their interactions with the androgen receptor have already been extensively studied and validated through both computational and experimental approaches.[35]

https://doi.org/10.1021/acs.est.5c10722
Environ. Sci. Technol. 2025, 59, 24323−24334

Therefore, our focus was directed toward investigating azole compounds with less well-characterized AR-binding profiles. To further estimate binding energies, we subjected the docked complexes to MM/GBSA analysis. Additionally, we performed pharmacokinetic and pharmacodynamic assessments, along with DFT calculations of azoles, to evaluate their physicochemical properties, toxicity, and reactivity.[19] Long-term MDSs were employed to assess the conformational and structural behavior as well as the stability of the azole-AR complexes. Post-MDS MM/GBSA analysis was conducted to estimate the binding affinities of azoles with AR, using various parameters. This computational analysis was complemented by experimental validation to visualize the interactions of azoles with AR and to better understand their toxicity.[33,44]

Molecular docking studies revealed that flusilazole, epoxiconazole, fenbuconazole, triflumizole, metconazole, and tebuconazole exhibited higher binding affinities with AR compared with other azoles. ADMET analysis was conducted to evaluate the pharmacokinetic behavior and potential toxicity risks of the selected azoles. Given that this class of compounds is known to exhibit toxicological effects, characterizing their absorption, distribution, metabolism, excretion, and toxicity profiles is essential for comprehensive risk assessment.[20,29] Predictions indicated a favorable oral absorption for these compounds. Notably, the toxicity screening revealed potential hepatotoxicity for several azoles including tebuconazole, triadimefon, tricyclazole, tebufenpyrad, carbendazim, cafenstrole, and benomyl. Although not the primary focus of this study, this finding is significant as it suggests that these compounds may pose additional health risks beyond endocrine disruption. This comprehensive profiling is vital for prioritizing azoles for further regulatory scrutiny and highlights the multifaceted toxicity inherent in this class of chemicals. DFT analysis was conducted to explore the chemical reactivity of the six azoles with the highest affinity for AR, predicting their enhanced reactivity, which is favorable for interaction with AR. Moreover, MD simulations and MM/GBSA calculations confirmed the stability and binding energy of the top screened azoles with AR. Additionally, the inconsistency observed between molecular docking and MM/GBSA results may be due to differences in their scoring functions and evaluation criteria, as has also been reported in previous studies.[19,45] However, the binding affinity of DHT for AR remains higher than that of the azoles as DHT is the natural ligand of AR. These findings suggest that azoles can disrupt the AR function. It is therefore plausible to hypothesize that continuous environmental exposure to these compounds may disrupt the normal functions of AR and interfere with DHT-AR interactions in vivo, potentially leading to various physiological dysfunctions. Future studies employing chronic, low-dose in vivo models are necessary to confirm this hypothesis.[4]

To ensure that the observed antagonistic effects on AR signaling were not confounded by nonspecific cytotoxicity, all functional assays were performed using the highest concentrations that maintained ≥80% cell viability, as recommended by OECD Test Guideline No. 458. Cell viability was measured in parallel with BRET assays, and only noncytotoxic concentrations were subsequently applied to quantitative real-time PCR and Western blot. The consistent inhibition of DHT-induced AR dimerization and expression under these conditions supports the conclusion that the tested azoles act as specific AR antagonists rather than general cytotoxins. An interesting observation was the discrepancy between the high computational binding affinity predicted for metconazole and its relatively moderate inhibitory efficacy in the cellular assays (BRET, qPCR, and Western blot). This suggests that high binding affinity alone may not directly translate to potent functional antagonism in a cellular context. The DFT calculations revealed that metconazole has a large HOMO−LUMO gap (6.10 eV), indicative of high chemical stability and lower reactivity. It is plausible that this stability influences its ability to induce the specific conformational change in AR required for effective antagonism, which may differ from azoles with narrower energy gaps, for example, triflumizole. Furthermore, complex cellular factors not accounted for in the in silico models such as differential cellular permeability, metabolic conversion, or interactions with transcriptional coregulators could also account for these differences. This highlights the critical importance of complementing computational predictions with experimental validation in a biologically relevant system.

Previous research has highlighted the toxic effects of several azoles studied herein, including flusilazole, epoxiconazole, fenbuconazole, triflumizole, metconazole, and tebuconazole. Specifically, flusilazole, epoxiconazole, triflumizole, and tebuconazole have been identified as AR antagonists.[46−49] These compounds were found to inhibit AR homodimerization in the cytosol due to their binding affinity for AR.[4] Additionally, metconazole was shown to disrupt the homodimerization of human androgen receptors, effectively suppressing androgen-induced transcriptional activation.[5] In contrast, fenbuconazole significantly impaired mitochondrial function and locomotor activity in zebrafish; at higher concentrations, it caused malformations and reduced activity. Its interference with mitochondrial respiration and strong binding to complex III highlight its potential toxicity to aquatic life.[50]

Given the frequent detection of these azoles in environmental samples such as surface waters, soils, and agricultural systems,[12,51] their potential to interact with human endocrine pathways including the AR, as demonstrated here, is a significant environmental health consideration. Investigating the interaction patterns and mechanisms of azoles with AR is a crucial area of research. This study is particularly important in an era where concerns about human, animal, and environmental health are increasingly recognized.[5] This research not only explores the interactions and toxicity of azoles but also addresses broader issues such as potential reproductive health effects that have gained global attention. By unraveling the intricate interactions between these compounds and AR using multiscale computational approaches, including molecular docking, ADMET prediction, DFT calculations, MDS, MM/GBSA calculations, and extensive experimental investigations, this study provides vital insights for the scientific community, policy-making, and real-world applications.[20,52]

This research provides valuable insights into the toxicity of azoles and identifies key amino acid residues in AR that are involved in their binding interactions. By shedding light on these critical aspects, this study paves the way for more in-depth investigations of azole toxicity. To the best of our knowledge, this study is the first to document the interaction between various azoles and AR. These findings are significant for advancing scientific understanding and could inform the development of new regulations aimed at protecting environmental health.

https://doi.org/10.1021/acs.est.5c10722
Environ. Sci. Technol. 2025, 59, 24323−24334

■ ASSOCIATED CONTENT

Supporting Information

The Supporting Information is available free of charge at https://pubs.acs.org/doi/10.1021/acs.est.5c10722.

Effect on dimerization of ligand-bound ARs in cytoplasm; determination of AR protein expression; assessment of pharmacokinetic profiles of azoles using different parameters; predicted toxicity profiles of azoles across different parameters; suppressing effects of six azoles on DHT-induced dimerization of cytosolic ARs; 2D diagrams illustrating the interactions of azoles with AR; comparison of energy levels for the HOMO, LUMO, and the energy gap in azoles; chemical reactivity analysis using DFT calculations and visualization of HOMO and LUMO orbitals for azoles with respect to DHT; protein−ligand interactions observed during the simulation; and interactions between amino acid residues of the AR and azoles plotted relative to DHT (PDF)

■ AUTHOR INFORMATION

Corresponding Authors

Hee-Seok Lee − *GreenTech-based Food Safety Research Group, BK21 Four, Department of Food Science and Biotechnology, Chung-Ang University, Anseong-si, Gyeonggi-do 17546, Republic of Korea;* orcid.org/0000-0002-6691-0096; Email: hslee0515@cau.ac.kr

Jun-Mo Kim − *Department of Animal Science and Technology, Chung-Ang University, Anseong-si, Gyeonggi-do 17546, Republic of Korea;* orcid.org/0000-0002-6934-398X; Email: junmokim@cau.ac.kr

Authors

Rajesh Kumar Pathak − *Department of Chemical Engineering, University of Rovira i Virgili, Tarragona 43007, Spain;* orcid.org/0000-0003-3835-8430

Da-Hyun Jeong − *GreenTech-based Food Safety Research Group, BK21 Four, Department of Food Science and Biotechnology, Chung-Ang University, Anseong-si, Gyeonggi-do 17546, Republic of Korea;* orcid.org/0000-0002-4352-4678

Min-Jae Jang − *Department of Animal Science and Technology, Chung-Ang University, Anseong-si, Gyeonggi-do 17546, Republic of Korea*

Complete contact information is available at: https://pubs.acs.org/10.1021/acs.est.5c10722

Author Contributions

R.K.P.: conceptualization, methodology, software, formal analysis, writing—original draft, and writing—review and editing. D.-H.J.: conceptualization, methodology, formal analysis, and validation. M.-J.J.: writing—review and editing. H.-S.L.: conceptualization, resources, supervision, and writing—review and editing. J.-M.K.: conceptualization, resources, supervision, writing—review and editing, project administration, and funding acquisition.

Notes

The authors declare no competing financial interest.

■ ACKNOWLEDGMENTS

This study was supported by the Basic Science Research Program through the National Research Foundation of Korea (NRF), funded by the Ministry of Education (RS-2018-NR031061). We gratefully acknowledge Chung-Ang University for providing high-performance computing resources and other essential facilities. The authors sincerely thank the peer reviewers for their constructive feedback, which improved the readability and overall quality of the manuscript.

■ REFERENCES

(1) Animasaun, D. A.; Adedibu, P. A.; Shkryl, Y.; Emmanuel, F. O.; Tekutyeva, L.; Balabanova, L. Modern Plant Biotechnology: An Antidote against Global Food Insecurity. *Agronomy* **2023**, *13* (8), 2038.

(2) Warner, G. R.; Mourikes, V. E.; Neff, A. M.; Brehm, E.; Flaws, J. A. Mechanisms of Action of Agrochemicals Acting as Endocrine Disrupting Chemicals. *Mol. Cell. Endocrinol.* **2020**, *502*, 110680.

(3) Nicolopoulou-Stamati, P.; Maipas, S.; Kotampasi, C.; Stamatis, P.; Hens, L. Chemical Pesticides and Human Health: The Urgent Need for a New Concept in Agriculture. *Front. Public Health* **2016**, *4*, 178764.

(4) Jung, D. W.; Jeong, D. H.; Lee, H. S. Endocrine Disrupting Potential of Selected Azole and Organophosphorus Pesticide Products through Suppressing the Dimerization of Human Androgen Receptor in Genomic Pathway. *Ecotoxicol. Environ. Saf.* **2022**, *247*, 114246.

(5) Jung, D. W.; Jeong, D. H.; Kim, U. J.; Lee, H. S. The Triazole Fungicide Metconazole Inhibits the Homodimerization of Human Androgen Receptors to Suppress Androgen-Induced Transcriptional Activation. *Chem. Biol. Interact.* **2023**, *378*, 110489.

(6) Sang, J.; Wang, H.; Yu, Y.; Ji, Z.; Xia, M.; Hao, T.; Li, L.; Ge, R. s. Azole Fungicides Inhibit Human and Rat Gonadal 3β-Hydroxysteroid Dehydrogenases: Structure-Activity Relationship and in Silico Docking Analysis. *Food Chem. Toxicol.* **2023**, *180*, 114028.

(7) Jørgensen, L. N.; Heick, T. M. Azole Use in Agriculture, Horticulture, and Wood Preservation − Is It Indispensable? *Front. Cell. Infect. Microbiol.* **2021**, *11*, 730297.

(8) Pintye, A.; Bacsó, R.; Kovács, G. M. Trans-Kingdom Fungal Pathogens Infecting Both Plants and Humans, and the Problem of Azole Fungicide Resistance. *Front. Microbiol.* **2024**, *15*, 1354757.

(9) Price, C. L.; Parker, J. E.; Warrilow, A. G.; Kelly, D. E.; Kelly, S. L. Azole Fungicides − Understanding Resistance Mechanisms in Agricultural Fungal Pathogens. *Pest Manag. Sci.* **2015**, *71* (8), 1054−1058.

(10) Zhang, F.; Zhou, D.; Kao, Y. C.; Ye, J.; Chen, S. Expression and Purification of a Recombinant Form of Human Aromatase from Escherichia Coli. *Biochem. Pharmacol.* **2002**, *64* (9), 1317−1324.

(11) Draskau, M. K.; Boberg, J.; Taxvig, C.; Pedersen, M.; Frandsen, H. L.; Christiansen, S.; Svingen, T. In Vitro and in Vivo Endocrine Disrupting Effects of the Azole Fungicides Triticonazole and Flusilazole. *Environ. Pollut.* **2019**, *255* (Pt 2), 113309.

(12) Draskau, M. K.; Svingen, T. Azole Fungicides and Their Endocrine Disrupting Properties: Perspectives on Sex Hormone-Dependent Reproductive Development. *Front. Toxicol.* **2022**, *4*, 883254.

(13) Fisher, M. C.; Alastruey-Izquierdo, A.; Berman, J.; Bicanic, T.; Bignell, E. M.; Bowyer, P.; Bromley, M.; Brüggemann, R.; Garber, G.; Cornely, O. A.; Gurr, S. J.; Harrison, T. S.; Kuijper, E.; Rhodes, J.; Sheppard, D. C.; Warris, A.; White, P. L.; Xu, J.; Zwaan, B.; Verweij, P. E. Tackling the Emerging Threat of Antifungal Resistance to Human Health. *Nat. Rev. Microbiol.* **2022**, *20* (9), 557−571.

(14) Fraaije, B. A.; Atkins, S. L.; Santos, R. F.; Hanley, S. J.; West, J. S.; Lucas, J. A. Epidemiological Studies of Pan-Azole Resistant Aspergillus Fumigatus Populations Sampled during Tulip Cultivation Show Clonal Expansion with Acquisition of Multi-Fungicide Resistance as Potential Driver. *Microorganisms* **2021**, *9* (11), 2379.

(15) Voiculescu, D. I.; Roman, D. L.; Ostafe, V.; Isvoran, A. A Cheminformatics Study Regarding the Human Health Risks Assess-

ment of the Stereoisomers of Difenoconazole. *Molecules* **2022**, *27* (15), 4682.
(16) Proença, S.; Escher, B. I.; Fischer, F. C.; Fisher, C.; Grégoire, S.; Hewitt, N. J.; Nicol, B.; Paini, A.; Kramer, N. I. Effective Exposure of Chemicals in in Vitro Cell Systems: A Review of Chemical Distribution Models. *Toxicol. in Vitro* **2021**, *73*, 105133.
(17) Forest, V. Experimental and Computational Nanotoxicology-Complementary Approaches for Nanomaterial Hazard Assessment. *Nanomaterials* **2022**, *12* (8), 1346.
(18) Jia, X.; Wang, T.; Zhu, H. Advancing Computational Toxicology by Interpretable Machine Learning. *Environ. Sci. Technol.* **2023**, *57* (46), 17690−17706.
(19) Pathak, R. K.; Kim, J. M. Structural Insight into the Mechanisms and Interacting Features of Endocrine Disruptor Bisphenol A and Its Analogs with Human Estrogen-Related Receptor Gamma. *Environ. Pollut.* **2024**, *345*, 123549.
(20) Pathak, R. K.; Jung, D. W.; Shin, S. H.; Ryu, B. Y.; Lee, H. S.; Kim, J. M. Deciphering the Mechanisms and Interactions of the Endocrine Disruptor Bisphenol A and Its Analogs with the Androgen Receptor. *J. Hazard. Mater.* **2024**, *469*, 133935.
(21) Chung, E.; Wen, X.; Jia, X.; Ciallella, H. L.; Aleksunes, L. M.; Zhu, H. Hybrid Non-Animal Modeling: A Mechanistic Approach to Predict Chemical Hepatotoxicity. *J. Hazard. Mater.* **2024**, *471*, 134297.
(22) Sen, P.; Vijay, M.; Singh, S.; Hameed, S.; Vijayaraghvan, P. Understanding the Environmental Drivers of Clinical Azole Resistance in Aspergillus Species. *Drug Target Insights* **2022**, *16* (1), 25−35.
(23) Xie, Y.; Li, J.; Salamova, A.; Zheng, G. Occurrence of Current-Use Pesticides in Paired Indoor Dust, Drinking Water, and Urine Samples from the United States: Risk Prioritization and Health Implications. *Environ. Sci. Technol.* **2025**, *59* (25), 12507−12519.
(24) Qin, L. T.; Tian, X. F.; Zhang, J. Y.; Liang, Y. P.; Zeng, H. H.; Mo, L. Y. A Comprehensive Machine Learning-Based Models for Predicting Mixture Toxicity of Azole Fungicides toward Algae (Auxenochlorella Pyrenoidosa). *Environ. Int.* **2024**, *194*, 109162.
(25) Schrödinger, L. *Schrödinger Release 2023-4*; Schrödinger, LLC: New York, NY, 2023.
(26) Lu, C.; Wu, C.; Ghoreishi, D.; Chen, W.; Wang, L.; Damm, W.; Ross, G. A.; Dahlgren, M. K.; Russell, E.; Von Bargen, C. D.; Abel, R.; Friesner, R. A.; Harder, E. D. OPLS4: Improving Force Field Accuracy on Challenging Regimes of Chemical Space. *J. Chem. Theory Comput.* **2021**, *17* (7), 4291−4300.
(27) Estébanez-Perpiñá, E.; Moore, J. M. R.; Mar, E.; Delgado-Rodrigues, E.; Nguyen, P.; Baxter, J. D.; Buehrer, B. M.; Webb, P.; Fletterick, R. J.; Guy, R. K. The Molecular Mechanisms of Coactivator Utilization in Ligand-Dependent Transactivation by the Androgen Receptor. *J. Biol. Chem.* **2005**, *280* (9), 8060−8068.
(28) Friesner, R. A.; Banks, J. L.; Murphy, R. B.; Halgren, T. A.; Klicic, J. J.; Mainz, D. T.; Repasky, M. P.; Knoll, E. H.; Shelley, M.; Perry, J. K.; Shaw, D. E.; Francis, P.; Shenkin, P. S. Glide: A New Approach for Rapid, Accurate Docking and Scoring. 1. Method and Assessment of Docking Accuracy. *J. Med. Chem.* **2004**, *47* (7), 1739−1749.
(29) Pires, D. E. V.; Blundell, T. L.; Ascher, D. B. PkCSM: Predicting Small-Molecule Pharmacokinetic and Toxicity Properties Using Graph-Based Signatures. *J. Med. Chem.* **2015**, *58* (9), 4066−4072.
(30) Bochevarov, A. D.; Harder, E.; Hughes, T. F.; Greenwood, J. R.; Braden, D. A.; Philipp, D. M.; Rinaldo, D.; Halls, M. D.; Zhang, J.; Friesner, R. A. J. Jaguar: A high-performance quantum chemistry software program with strengths in life and materials sciences. *Int. J. Quantum Chem.* **2013**, *113* (18), 2110−2142.
(31) Jorgensen, W. L.; Chandrasekhar, J.; Madura, J. D.; Impey, R. W.; Klein, M. L. Comparison of Simple Potential Functions for Simulating Liquid Water. *J. Chem. Phys.* **1983**, *79* (2), 926−935.
(32) Yazdani, B.; Sirous, H.; Brogi, S.; Calderone, V. Structure-Based High-Throughput Virtual Screening and Molecular Dynamics Simulation for the Discovery of Novel SARS-CoV-2 NSP3Mac1 Domain Inhibitors. *Viruses* **2023**, *15* (12), 2291.
(33) Lee, S. H.; Hong, K. Y.; Seo, H.; Lee, H. S.; Park, Y. Mechanistic Insight into Human Androgen Receptor-Mediated Endocrine-Disrupting Potentials by a Stable Bioluminescence Resonance Energy Transfer-Based Dimerization Assay. *Chem. Biol. Interact.* **2021**, *349*, 109655.
(34) OECD. *Test No. 458: Stably Transfected Human Androgen Receptor Transcriptional Activation Assay for Detection of Androgenic Agonist and Antagonist Activity of Chemicals*. 2023. DOI: .
(35) Jeong, D. H.; Pathak, R. K.; Jung, D. W.; Kim, J. M.; Lee, H. S. Exploring the Relationship between the Androgen Receptor and Structural Configuration of Benzophenones: A Combination of Computational Analysis and Laboratory Models. *Environ. Int.* **2025**, *202*, 109632.
(36) Lee, H. S.; Lee, S. H.; Park, Y. Enhancement of Androgen Transcriptional Activation Assay Based on Genome Edited Glucocorticoid Knock out Human Prostate Cancer Cell Line. *Environ. Res.* **2019**, *171*, 437−443.
(37) Castelo-Branco, D.; Lockhart, S. R.; Chen, Y. C.; Santos, D. A.; Hagen, F.; Hawkins, N. J.; Lavergne, R. A.; Meis, J. F.; Le Pape, P.; Rocha, M. F. G.; Sidrim, J. J. C.; Arendrup, M.; Morio, F. Collateral Consequences of Agricultural Fungicides on Pathogenic Yeasts: A One Health Perspective to Tackle Azole Resistance. *Mycoses* **2022**, *65* (3), 303−311.
(38) Johansson, H. K. L.; Christiansen, S.; Draskau, M. K.; Svingen, T.; Boberg, J. Classical Toxicity Endpoints in Female Rats Are Insensitive to the Human Endocrine Disruptors Diethylstilbestrol and Ketoconazole. *Reprod. Toxicol.* **2021**, *101*, 9−17.
(39) Melching-Kollmuss, S.; Fussell, K. C.; Schneider, S.; Buesen, R.; Groeters, S.; Strauss, V.; van Ravenzwaay, B. Comparing Effect Levels of Regulatory Studies with Endpoints Derived in Targeted Anti-Androgenic Studies: Example Prochloraz. *Arch. Toxicol.* **2017**, *91* (1), 143−162.
(40) Schwartz, C. L.; Christiansen, S.; Hass, U.; Ramhøj, L.; Axelstad, M.; Löbl, N. M.; Svingen, T. On the Use and Interpretation of Areola/Nipple Retention as a Biomarker for Anti-Androgenic Effects in Rat Toxicity Studies. *Front. Toxicol.* **2021**, *3*, 730752.
(41) Wu, W.; Jiang, T.; Lin, H.; Chen, C.; Wang, L.; Wen, J.; Wu, J.; Deng, Y. The Specific Binding and Promotion Effect of Azoles on Human Aldo-Keto Reductase 7A2. *Metabolites* **2023**, *13* (5), 601.
(42) Munkboel, C. H.; Rasmussen, T. B.; Elgaard, C.; Olesen, M. L. K.; Kretschmann, A. C.; Styrishave, B. The Classic Azole Antifungal Drugs Are Highly Potent Endocrine Disruptors in Vitro Inhibiting Steroidogenic CYP Enzymes at Concentrations Lower than Therapeutic Cmax. *Toxicology* **2019**, *425*, 152247.
(43) Townsend, P. A.; Grayson, M. N. Density Functional Theory in the Prediction of Mutagenicity: A Perspective. *Chem. Res. Toxicol.* **2021**, *34* (2), 179−188.
(44) Uesawa, Y. Efficiency of Pharmaceutical Toxicity Prediction in Computational Toxicology. *Toxicol. Res.* **2024**, *40* (1), 1−9.
(45) Hou, T.; Wang, J.; Li, Y.; Wang, W. Assessing the Performance of the Molecular Mechanics/Poisson Boltzmann Surface Area and Molecular Mechanics/Generalized Born Surface Area Methods. II. The Accuracy of Ranking Poses Generated from Docking. *J. Comput. Chem.* **2011**, *32* (5), 866−877.
(46) Pedersen, E. B.; Christiansen, S.; Svingen, T. AOP Key Event Relationship Report: Linking Androgen Receptor Antagonism with Nipple Retention. *Curr. Res. Toxicol.* **2022**, *3*, 100085.
(47) Kjærstad, M. B.; Taxvig, C.; Nellemann, C.; Vinggaard, A. M.; Andersen, H. R. Endocrine Disrupting Effects in Vitro of Conazole Antifungals Used as Pesticides and Pharmaceuticals. *Reprod. Toxicol.* **2010**, *30* (4), 573−582.
(48) Álvarez, F.; Arena, M.; Auteri, D.; Binaglia, S. B. L. M.; Castoldi, A. F.; Chiusolo, A.; Colagiorgi, A.; Colas, M.; Crivellente, F.; De Lentdecker, C.; De Magistris, I.; Egsmose, M.; Fait, G.; Ferilli, F.; Gouliarmou, V.; Halling, K.; Nogareda, L. H.; Ippolito, A.; Istace, F.; Jarrah, S.; Kardassi, D.; Kienzler, A.; Lanzoni, A.; Lava, R.; Leuschner, R.; Linguadoca, A.; Louisse, J.; Lythgo, C.; Magrans, O.; Mangas, I.;

Miron, I.; Molnar, T.; Padovani, L.; Padricello, V.; Panzarea, M.; Morte, J. M. P.; Rizzuto, S.; Romac, A.; Rortais, A.; Serafimova, R.; Sharp, R.; Szentes, C.; Terron, A.; Theobald, A.; Tiramani, M.; Vianello, G.; European Food Safety Authority EFSA; et al. Peer Review of the Pesticide Risk Assessment of the Active Substance Metconazole. *EFSA J.* **2023**, *21* (8), No. e08141.

(49) Bever, R. J.; Edwards, S. W.; Antonijevic, T.; Nelms, M. D.; Ring, C.; Harris, D.; Lynn, S. G.; Williams, D.; Chappell, G.; Boyles, R.; Borghoff, S.; Markey, K. J. Optimizing Androgen Receptor Prioritization Using High-Throughput Assay-Based Activity Models. *Front. Toxicol.* **2024**, *6*, 1347364.

(50) Qin, Y.; Wang, X.; Yan, X.; Zhu, D.; Wang, J.; Chen, S.; Wang, S.; Wen, Y.; Martyniuk, C. J.; Zhao, Y. Developmental Toxicity of Fenbuconazole in Zebrafish: Effects on Mitochondrial Respiration and Locomotor Behavior. *Toxicology* **2022**, *470*, 153137.

(51) Zarn, J. A.; Brüschweiler, B. J.; Schlatter, J. R. Azole Fungicides Affect Mammalian Steroidogenesis by Inhibiting Sterol 14 Alpha-Demethylase and Aromatase. *Environ. Health Perspect.* **2003**, *111* (3), 255−261.

(52) Barber, C.; Fowkes, A.; Hanser, T.; Heghes, C. From Model Performance to Decision Support − The Rise of Computational Toxicology in Chemical Safety Assessments. *Comput. Toxicol.* **2024**, *31*, 100303.



https://doi.org/10.1021/acs.est.5c10722
Environ. Sci. Technol. 2025, 59, 24323−24334